Molecular Crystals and Liquid Crystals Science and Technology. Section A. Molecular Crystals and Liquid Crystals

Publication details, including instructions for authors and subscription information:
http://www.tandfonline.com/loi/gmcl19

Homeotropic to Twisted Planar Transition in Nematic Liquid Crystals with Negative Dielectric Amsotropy

Seong-Woo Suh [a], Sung Tae Shin [a b] & Sin-Doo Lee [a]

[a] Physics Department, Sogang University, C. P. O. Box 1142, Seoul, Korea

[b] Samsung Electronics Co. Ltd., Kiheung, Yongin, Kyungki, Korea

Version of record first published: 04 Oct 2006

To cite this article: Seong-Woo Suh, Sung Tae Shin & Sin-Doo Lee (1997): Homeotropic to Twisted Planar Transition in Nematic Liquid Crystals with Negative Dielectric Amsotropy, Molecular Crystals and Liquid Crystals Science and Technology. Section A. Molecular Crystals and Liquid Crystals, 302:1, 163-168

To link to this article: http://dx.doi.org/10.1080/10587259708041824

Mol. Cryst. Liq. Cryst., 1997, Vol. 302, pp. 163–168
Reprints available directly from the publisher
Photocopying permitted by license only

HOMEOTROPIC TO TWISTED PLANAR TRANSITION IN NEMATIC LIQUID CRYSTALS WITH NEGATIVE DIELECTRIC ANISOTROPY

SEONG-WOO SUH, SUNG TAE SHIN,† and SIN-DOO LEE*
Physics Department, Sogang University, C. P. O. Box 1142, Seoul, Korea
†Samsung Electronics Co. Ltd., Kiheung, Yongin, Kyungki, Korea

Abstract We have studied the effect of molecular chirality and cell gap on the electro-optic (EO) modulation associated with a homeotropic to twisted-planar (HTP) transition. It is found that an optimum condition of the cell gap and the corresponding chirality exists for the maximum EO modulation. A surface layer of the HTP structure is somewhat thicker than that of a conventional twisted nematic one. The helical pitch predominantly governs waveguiding characteristics and the resultant EO properties of the HTP structure. The polar and azimuthal surface anchoring on treated homeotropic alignment layers is also discussed.

INTRODUCTION

Among various electro-optic (EO) effects in nematic liquid crystals (NLCs), the twisted nematic (TN) one[1,2] has been extensively utilized for information displays and successfully applied to portable TVs and lap-top computers, especially in thin-film transistor(TFT) addressing scheme. However, the TN effect using positive dielectric anisotropy of NLCs with homogeneous alignment has several shortcomings such as limited display contrast and narrow viewing characteristics. Another EO effect using negative dielectric anisotropy of NLCs with homeotropic alignment is often called deformation of vertical aligned phases or electrically controlled birefringence mode.[3,4]

Very recently, we have reported a novel EO effect, associated with a homeotropic to twisted planar (HTP) structural transition, in NLCs with negative dielectric anisotropy and molecular chirality.[5] With the help of an external twist generated by rubbing and proper molecular chirality, the helical structure is formed in a field-on state of the HTP cell. The field-on state behaves as a polarization rotator in the waveguiding regime. In this regime, the optical transmission through the HTP cell is fairly insensitive to the wavelength of the incident light. Moreover, the HTP structure has high contrast and good viewing characteristics required for high quality displays.

In the present work, we have studied the EO properties of HTP as a function of molecular chirality and cell gap. From both the experimental and numerical results, the control of molecular chirality and the cell gap is found to play an important role in optimizing the HTP architecture. Several material parameters are deduced from theoretical fits of the experimental data within the continuum description.

EXPERIMENTAL

A commercial mixture, EN-37 of Chisso Petrochemical Corp., was used as a host NLC with negative dielectric anisotropy. The chiral additive used was S-811 of E. Merck. Various HTP cells of different gaps and doping ratio of S-811 were used in this study. The homeotropic alignment layer was prepared with JALS-203 of Japan Synthetic Rubber Co., followed by rubbing to break the azimuthal symmetry for the HTP structural transition under an external electric field. The HTP cell was assembled such that the twist angle between the rubbing axes on two surfaces makes 90°. For the EO measurements, the HTP cell was placed under crossed polarizers which coincide with the rubbing axes. A He-Ne laser of 632.8 nm was used as a light source. A square wave voltage at 1 kHz, generated from an arbitrary waveform generator, was applied to the cell. The transmitted intensity was monitored with a photodiode in conjunction with a digitizing storage oscilloscope and a digital multimeter. All measurements were carried out at room temperature.

RESULTS AND DISCUSSION

Fig. 1 shows the transmitted intensities through the HTP cells of various gaps as function of the applied voltage. For all cases, the amount of the chiral additive was adjusted to produce the ratio of the cell gap to pitch $d/p \approx 0.25$. The solid lines represent the least-square fits performed in the continuum theory. Details of a theoretical description will be discussed later on. As shown in Fig. 1, all the HTP cells studied possess the same threshold voltage. One interesting point is that an optimum cell gap ($\approx 7\mu$m) exists for the maximum EO modulation. For a relatively thin cell (4.5μm), the helical pitch corresponding to the twist of 90° should decrease. Therefore, waveguiding of an incident polarization is incomplete, and the optical transmission through the cell decreases. In fact, both the waveguiding and birefringence effects are responsible for the EO characteristics of the HTP cell. For a thick cell (10.4μm), however, the birefringence effect becomes dominant just above the threshold, which results in a peak in the optical transmission at around 3V. This peak can be described in terms of the twist distortions of the director with changing the electric field.

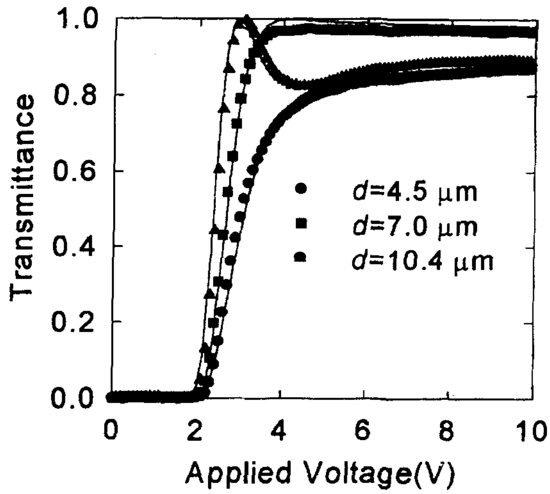

Figure 1: The transmitted intensity as a function of the applied voltage. The solid lines are the least-square fits performed with theoretical results.

The activated, field-on state of the HTP cell is very similar to the inactivated, field-off state of the TN one except for the surface region. The first maximum (or minimum) in the optical transmission through the inactivated 90° TN cell occurs at[6] $\Delta nd/\lambda = \sqrt{3}/2$ with Δn the birefringence and λ the wavelength of the incident light. In our case, the cell gap of 5.5μm satisfies this condition provided that $\Delta n = 0.1$ and $\lambda = 632.8$nm. Considering the fact that the homeotropically aligned surface region of the HTP cell is hardly transformed into a twisted-planar structure, it is not surprising that the optimum gap of 5.5μm for the TN cell is (10 $\sim$ 20 smaller than 7.0μm for the HTP case.

For numerical simulations, we adopt total free energy (F_{tot}) as a combination[7] of the elastic energy (F_e), dielectric energy (F_d), and surface energy (F_s). The surface energy of the rubbed JALS-203 alignment layer consists of the polar and azimuthal parts in the Rapini-Papoular form.[8]

$$\begin{aligned} F_{tot} &= \int_0^d dz\,(F_{el} + F_d) + F_s \\ &= \int_0^d \left[\frac{1}{2}K_1(\nabla\cdot\mathbf{n})^2 + \frac{1}{2}K_2(\mathbf{n}\cdot\nabla\times\mathbf{n} - q)^2 + \frac{1}{2}K_3(\mathbf{n}\times\nabla\times\mathbf{n})^2 \right. \\ &\qquad \left. - \frac{1}{2}\mathbf{D}\cdot\mathbf{E}\right] dz + W_p\sin^2\theta + W_a\sin^2\phi, \end{aligned} \tag{1}$$

where $\mathbf{n}$ denotes the director, θ the tit angle, ϕ the twist angle, and K_i (i=1,2, and 3) the elastic constants. Here, $\mathbf{E}$ and $\mathbf{D}$ are the electric field and displacement. W_p and W_a are polar and azimuthal anchoring energies, respectively. From the best fits in Fig. 1, we determined the elastic constants as $K_1 = 14.5 \times 10^{-12}$N, $K_2 = 6.2 \times 10^{-12}$N, and $K_3 = 12.7 \times 10^{-12}$N. Moreover, the ordinary and extraordinary refractive indices, $n_\perp$ and $n_\parallel$, are 1.486 and 1.391, respectively. This is consistent with the literature.

Fig. 2 shows the twist profile of the director in the 90° HTP cell as a function of the spatial coordinate at various voltages. Below the threshold voltage ($\approx$ 2V), no twist distortions are involved and the homeotropic alignment is preserved. Above the threshold, the molecules tend to orient perpendicular to the field because of the negative dielectric anisotropy. It should be noted that the surface tilt is hardly changed although the director experiences tilt distortions in the bulk.

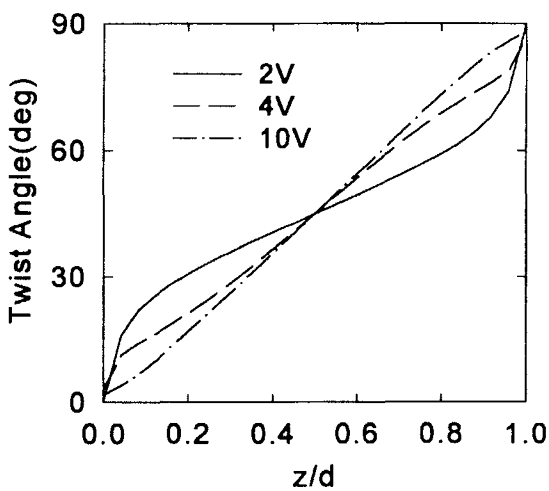

Figure 2: The twist profile of the director in the 90° HTP cell as a function of the spatial coordinate at various voltages.

In contrast to tilt distortions, twist distortions are strongly influenced by both the chirality introduced and the twist imposed on the cell surfaces during the HTP structural transition. Just above the threshold (2~4V), the birefringence effect becomes dominant than the waveguiding one in the bulk.

Now, we deal with the effect of the chirality on the resultant EO properties of the HTP cell of fixed gap $d = 4.5\mu$m. The amount of the chiral additive S-811 was varied. Fig. 3 shows the transmitted intensity through the HTP cell as function of the applied voltage. One interesting point is that the natural twist angle of around

90° is not the optimum case. As already shown in Fig. 1, for $d/p \approx 0.25$, the helical pitch less than 25μm will not fulfill the waveguiding condition. For a relatively thin cell, a less twisted structure exhibits rather larger transmission. Therefore, the HTP cell can be optimized using a proper cell gap and the corresponding d/p ratio for given Δn.

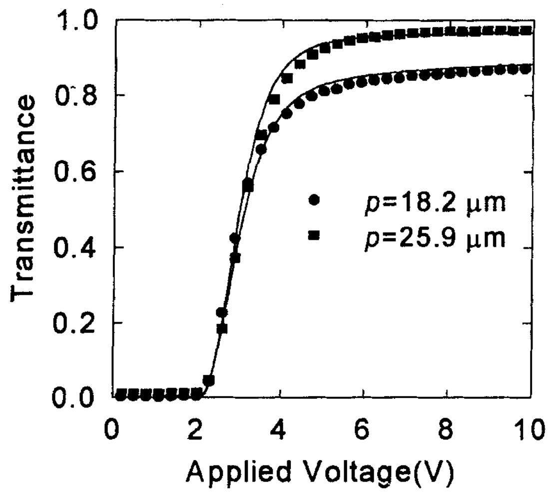

Figure 3: The transmitted intensity as a function of the applied voltage for two different helical pitches. The solid lines are the least-square fits to numerical simulations.

It has been reported[5] that the azimuthal anchoring of the the homeotropic alignment is the critical factor for stabilizing the HTP structure. While the polar anchoring determines the thickness of the surface layer, the azimuthal anchoring dictates the stability of the twist distortions during the HTP structural transition.

Table 1: Measured twist angle and azimuthal anchoring energy (W_a) in the HTP cell as a function of the pitch.

pitch(μm)	twist angle(deg)	W_a($\times 10^{-7}$N/m)
26.7	-122.3	3.0
35.3	-97.6	3.3
68.6	-63.9	3.2

The azimuthal anchoring energy is estimated[9] from the twist angle measured in an activated planar state in the high voltage limit. The measured twist angle and estimated azimuthal anchoring energy of the rubbed JALS-203 homeotropic layer are shown in Table 1. Three HTP cells, weakly rubbed, with different helical pitches were studied. The azimuthal anchoring energy was found to be about 3.0×10^{-7}N/m, which is nearly independent of the helical pitch. This value is somewhat smaller than that of a glass substrate ($\approx 7 \times 10^{-6}$N/m).[10] On the other hand, the measured polar anchoring energy was about 2.6×10^{-5}N/m, which is significantly larger than azimuthal one. It is generally believed that azimuthal anchoring is ($1 \sim 2$) order(s) of magnitude smaller than the polar one.

CONCLUSION

We have presented the experimental and theoretical results for the EO modulation associated with the HTP structural transition in NLCs with negative dielectric anisotropy. It was found that an optimum condition of the cell gap and the molecular chirality exists for the maximum EO modulation. The azimuthal anchoring of the rubbed homeotropic alignment layer plays an important role in the stability of the HTP structure and the reproducibility of the associated EO properties. Numerical simulations, performed within the continuum elastic formalism, describe well the main features of our experimental results.

ACKNOWLEDGMENT

This work was supported in part by the Ministry of Education of Korea through BSRI 96.

REFERENCES

1. M. Schadt and W. Helfrich, Appl. Phys. Lett. 18, 127 (1971).
2. M. Schadt, Mol. Cryst. Liq. Cryst. 165, 405 (1988).
3. M. F. Schiekel and K. Fahrenschon, Appl. Phys. Lett. 19, 391 (1971).
4. F. J. Kahn, G. N. Taylor, and H. Schonhorn, Proc. IEEE 61, 823 (1973).
5. S.-W. Suh, S. T. Shin, and S.-D. Lee, Appl. Phys. Lett. 68, 2819 (1996).
6. C. H. Gooch and H. A. Terry, J. Phys. D 8, 1575 (1975).
7. See for example, P. G. de Gennes and J. Prost, Physics of Liquid Crystals (Clarendon Press, Oxford, 1993).
8. A. Rapini and M. Papoular, J. Phys. (Paris) Colloq. 30, C4 (1969).
9. J. Min, H. Ximin, W. Zongkai, M. Kai, and Z. Xinyi, Liq. Cryst. 18, 419 (1995).
10. J. Sciart, J. Phys. (Paris) Lett. 37, L25 (1976).